

# An Application of Tomographic Reconstruction of Atmospheric CO<sub>2</sub> Over a Volcanic Site Based on Open-Path IR Laser Measurements

Claudio Belotti, Fabrizio Cuccoli, Luca Facheris, and Orlando Vaselli

**Abstract**—The southern area of Italy is characterized by the presence of many active volcanic areas. In Pozzuoli (Naples, Italy), an urban area characterized by high volcanic risk, a gas emitting site is present. An high percentage of CO<sub>2</sub> is emitted, whose atmospheric concentration measurement is an important task in many environmental and scientific applications. In this paper, we describe the utilization over that area of a mobile infrared (IR) laser system, able to measure the CO<sub>2</sub> concentration along rectilinear atmospheric paths up to 1-km length, and the result of tomographic processing applied to retrieve a two-dimensional CO<sub>2</sub> concentration field. The laser system computes the link averaged concentration by processing the received IR laser radiation propagated along an open-air rectilinear link connecting the transmitter/receiver laser unit and a passive retroreflector device. A one-day measurement campaign has been made and 15 different atmospheric propagation links were considered moving the transmitter/receiver unit and some retroreflectors.

**Index Terms**—Diode laser, tomography, carbon dioxide (CO<sub>2</sub>), air remote sensing.

## I. INTRODUCTION

IN RECENT YEARS, some work was published concerning the use of different tomographic approaches based on simple smooth functions, and different measurement systems/methods for retrieving two-dimensional (2-D) distributions of air gaseous components. For instance, in [1] was proposed the use of smooth basis functions minimization (SBFM) and applied to open path-Fourier transform infrared spectrometer (OP-FTIR) measurements in indoor SF<sub>6</sub> air monitoring. In [2], it was shown (through simulations) that an outdoor 2-D distribution of atmospheric components can be retrieved adopting a stochastic tomographic procedure [stochastic reconstruction technique (SRT)] exploiting laser attenuation measurements made along a number of rectilinear propagation paths defined by transmitter-retroreflector-receiver systems operating in the infrared (IR) region. As explained in [2], by accurately selecting the IR laser wavelength, it is possible to utilize laser attenuation measurements along a linear open-path to retrieve the number of molecules of a single species of interest along such path.

Manuscript received September 6, 2002; revised March 10, 2003. This work was supported in part by the Italian Space Agency (ASI).

C. Belotti, F. Cuccoli, and L. Facheris are with the Department of Electronics and Telecommunications and the Consorzio Nazionale Interuniversitario delle Telecomunicazioni (CNIT), 50139 Florence, Italy (e-mail: cuccoli@achille.det.unifi.it; facheris@ingfi1.ing.unifi.it).

O. Vaselli is with the Department of Earth Sciences, University of Florence, 50121 Florence, Italy (e-mail: orlando@steno.geo.unifi.it).

Digital Object Identifier 10.1109/TGRS.2003.815400



Fig. 1. Picture of the campaign site: "Solfatara di Pozzuoli," Pozzuoli (Naples), Italy.

Similar measurements made along different coplanar paths define a coverage area where, through the cited tomographic processing, it is possible to retrieve the 2-D concentration of that species. The major concern of the approach discussed in [2] is to retrieve as much information as possible about the 2-D molecular concentration of atmospheric components by utilizing a limited number of IR links, in order to minimize the outdoor instrumentation complexity and the total acquisition time. Obviously, the choice of using a limited number of links not only increases the ill-conditioning of the inversion problem, but intrinsically limits the spatial resolution: this can be acceptable for remote sensing applications in dangerous or not easily accessible sites (volcanic areas, industrial plants), where it may be difficult or impossible to adopt an experimental setup like that described in [1], that would indeed guarantee a greater spatial resolution.

In this paper, the theoretical concepts described in [2] are applied to a set of experimental data gathered during a measurement campaign made to retrieve the concentration field of atmospheric CO<sub>2</sub> over a volcanic area using a specific IR laser apparatus and a set of retroreflectors. The monitored area (Fig. 1) is the "Solfatara" in Pozzuoli (Naples, Italy): it has been chosen for its remarkable CO<sub>2</sub> emission, whose concentration control is also important for safety reasons [3], [4]. The IR laser system used in this one-day campaign is a transmitter/receiver unit, produced by Boreal Laser, Inc., that is able to measure the average concentration of CO<sub>2</sub> along an optical path between such unit and a passive retroreflector [5].

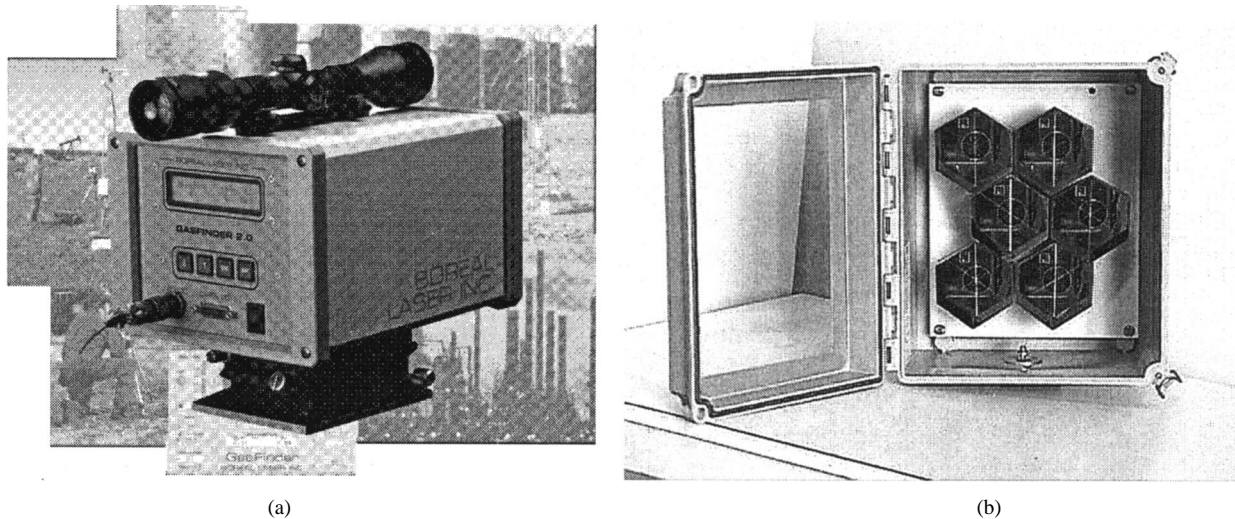


Fig. 2. (a) Gasfinder unit. (b) Six-piece corner cube retroreflector.

The measurement method used to provide such concentration (hereon referred to as linear concentration), described in Section 2, permits to perform  $\text{CO}_2$  measurements practically in real time: once the necessary set up operations required by the measurement apparatuses are made, the linear concentration measurement can be made in less than 1 s. The IR laser power characteristics are such that the maximum length of the optical path is about 1 km, and the minimum linear concentration value is 1000 ppm (parts per million per meter) in standard atmospheric conditions. This is sufficient to operate this kind of apparatuses in areas with extensions similar to that discussed here, but in general it is expected that performances of the measurement system degrade due to a (variable) number of disturbance sources that may be present in the volcanic environment.

The purpose of this paper is twofold: to present the approach and the results of the first experimental measurement campaign in a volcanic environment made with the IR apparatus described and to test the qualitative performance of tomographic processing for practical applications. For instance, since the result of tomographic data processing is the 2-D-concentration field of  $\text{CO}_2$  on a thin air layer (ideally, the plane surface where all the optical links lie) over some emitting sources, such estimated field may provide information on location and emission parameters of that source. In the experimental setup described here, since the position of the sources of  $\text{CO}_2$  in the monitored area are well known, comparing the position of the maxima in the reconstructed field of  $\text{CO}_2$  and the real positions of the emitting points permit a better discussion of the performance of the tomographic reconstruction. For such a purpose, it is of paramount importance that weather parameters be accurately analyzed and accounted for; therefore a portable meteorological station was used during all the measurement operations, measuring continuously air temperature, direction and speed of wind.

The paper is structured as follows. In Sections 1 and 2, the instrumentation utilized in the measurement campaign and the experimental setup are described, respectively, while Sections 3 and 4 are, respectively, devoted to the description and analysis

of the collected data, as well as to the results of tomographic processing.

## II. MEASUREMENT INSTRUMENTATION

The basic measurement apparatus is the  $\text{CO}_2$  Gasfinder [Fig. 2(a)], that is a IR laser transmitter/receiver unit. The laser source is a near-infrared room temperature tunable diode laser operating around 1580 nm, where the  $\text{CO}_2$  has a single absorption line [6]. A schematic representation of the main components of the Gasfinder unit is shown in Fig. 3.

The  $\text{CO}_2$  GasFinder [5] measures the  $\text{CO}_2$  concentration along the atmospheric optical path between the Gasfinder itself and a passive retroreflector [Fig. 2(b)]. The radiation emitted from the IR laser transmitter propagates through the atmosphere to the retroreflector and returns back to the receiver where it is focused onto a photodiode detector. Simultaneously, a portion of the IR laser beam passes through a reference cell contained in the Gasfinder unit, so as to provide a continuous calibration update. The reference cell has a stable  $\text{CO}_2$  reference concentration of known value.

The wavelength of the laser radiation is modulated in order to scan continuously the whole spectral range interested by the  $\text{CO}_2$  absorption line at 1580 nm. The wavelength modulation and the nonlinear effects of the radiation-matter interaction generates the second harmonic component.

The two second harmonic components of the signals received from the retroreflector and from the reference cell are converted into electrical waveforms that are then processed by the micro-controller to determine the actual linear concentration of the gas along the optical path. The Gasfinder can be set to provide a linear concentration value with variable time step, the minimum being 1 s. For each linear concentration measurement a confidence parameter R2—ranging between 0 and 1—is also provided, which is a reliability index: in fact, R2 is the correlation index between the two second harmonic components, the measurement reliability being maximum when  $R2 = 1$  [7], [8].

A quick alignment between the Gasfinder unit and the retroreflector is obtained through a red visible aiming laser and

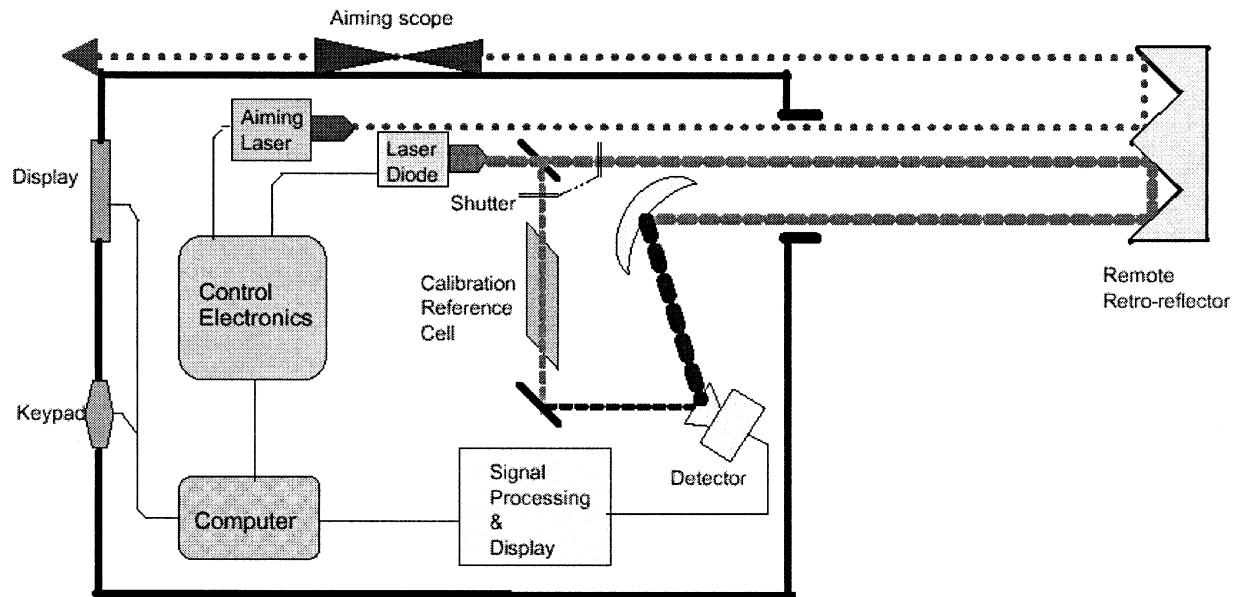


Fig. 3. Schematic representation of the components of the Gasfinder unit (from [5]).

a sighting scope. In general, the size of the retroreflector unit should be chosen based on the optical path length and on the expected amount of absorbed radiation. In this measurement campaign, we used retroreflectors like that shown in Fig. 3(b). The retroreflector is composed by six elements made by three faces of a vertex of a cube with 45-mm side. All faces are gold plated in order to reflect the IR radiation with maximum efficiency. The optical path distances were measured using an IR manual Rangefinder, that is able to provide the distance measurement up to about 500 m with 1-m resolution.

A portable meteorological station provided 1 minute averaged temperature, horizontal wind direction and speed. The temperature and wind speed resolutions are 0.1 °C and 0.1 m/s, respectively, while the angular resolution of the wind direction is 22.5°.

### III. MEASUREMENT CAMPAIGN

The measurement campaign was made on November 20, 2001 in the “Solfatara” area in Pozzuoli, in particular over an about 5000-m<sup>2</sup> area of the Solfatara characterized by the presence of some extremely active sources emission phenomena (see Fig. 1). A protection fence surrounds the emission area for safety reasons, since several emitted gases are toxic. Fig. 4 is a plane representation showing the position of the measurement network with respect to the gaseous emission area (shaded in gray). Two Gasfinder positions (marked with + markers in Fig. 4) were chosen, both outside the protection fence to minimize the permanence of the Gasfinder operator within the gray area. The plane surface of the tomographic network is located about 1.5 m over the terrain and the number of optical links utilized on the surface is 15. The portable weather station was placed in a fixed position (coordinates: (0 0) in Fig. 4) for the whole campaign.

The basic problem faced with the experimental setup was to have at disposal one Gasfinder unit and four retroreflectors, with the consequent need to “synthesize” the measurement net-

work by moving the retroreflectors and the Gasfinder around the monitored area in different time intervals. In order to minimize the time needed to change the position of the apparatus, we placed the Gasfinder in the first of the two positions, then we made the CO<sub>2</sub> measurements along links 1–6 moving the retroreflectors in sequence. While the Gasfinder was aiming at one retroreflector and acquiring data, we moved the other available retroreflectors to the subsequent positions. Successively, we moved the Gasfinder in the second position and the CO<sub>2</sub> measurements along links 7–15 were made following the same procedure for the alignments with retroreflectors and pertinent link measurements.

Interpreting the data collected in such a way is simple if made with reference to each single link, the basic problem being the variation of the atmospheric conditions, in particular wind speed and direction. For this reason, measurements along each link were made continuously, collecting one sample per s for total acquisition times ranging between 5 and 10 min, in order to gather the maximum amount of samples per link. The total acquisition time was decided by the operator link by link, depending on the current wind conditions. In fact, wind direction and speed influence directly atmospheric concentration of gaseous substances. The target of this measurement procedure was therefore to acquire a sufficient number of samples per link, in order to extract those with the same wind conditions. If found, such a subset of data could be interpreted as representative of a CO<sub>2</sub> concentration field in stationary wind conditions. Acting so, the whole measurement operations on the network were made in about 3 h and the time needed to change the optical alignment between the Gasfinder and one retroreflector—a few tens of seconds—could be considered negligible.

### IV. DATA REPORT

As mentioned, the whole collected dataset is composed of temperature, wind direction, and wind speed values collected in

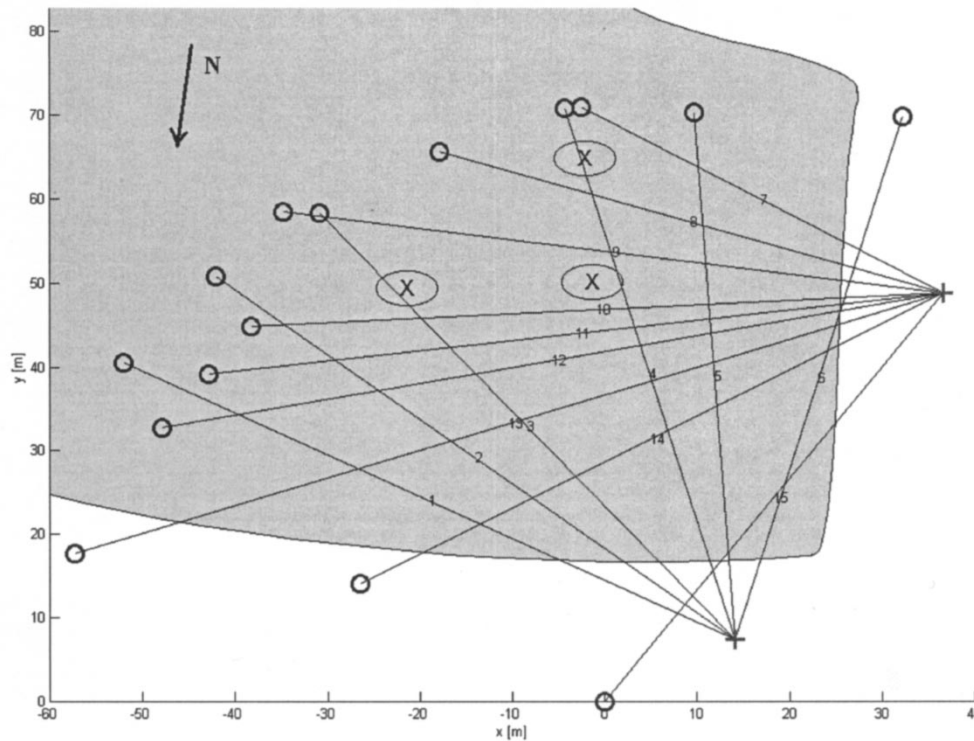


Fig. 4. Measurement links over the monitored area. The gray area is the restricted area (the contour is the protection fence). The + markers correspond to the two Gasfinder positions, the O markers to the retroreflector positions and the X markers to the main visible emission points. The meteorological station was placed in (0, 0) during the whole campaign. The north direction is indicated in the top left of figure.

a fixed location every minute, and the  $\text{CO}_2$  linear concentration with 1 s resolution for each link. The acquired meteorological parameters are shown in Fig. 5.

A compact report for the  $\text{CO}_2$  concentration measurements is shown in Table I. Each row of the table refers to one link of the measurement network shown in Fig. 4. The parameters reported in the table are as follows.

- A. **Number:** the link numbering follows that used in Fig. 4.
- B. **Length:** the optical path length (distance between the Gasfinder and the retroreflector).
- C. **Start time:** initial instant of the link data acquisition.
- D. **End time:** final instant of the link data acquisition.
- E. **Duration:** difference (in seconds) between the end time and the start time (D and C).
- F. **Number of samples:** number of valid data (we consider one  $\text{CO}_2$  linear concentration measurement as data valid if the relative confidence index  $R2 > 0.95$ ).
- G. **Mean linear concentration:** the mean value of the  $\text{CO}_2$  linear concentration data. Such mean value has been computed on the number of valid data (F column).
- H. **H1) (Mean concentration) and H2) (standard deviation):** the mean of the  $\text{CO}_2$  linear concentration data divided by the link length and its standard deviation.
- I. **Minimum concentration:** the minimum value of the  $\text{CO}_2$  linear concentration data divided by the link length.
- J. **Maximum concentration:** the maximum value of the  $\text{CO}_2$  linear concentration data divided by the link length.

The nonstationarity of wind, is evident: notice, however, that while wind speed was continuously changing, its direction was fortunately fairly uniform during the whole campaign. Such wind conditions, jointly with the turbulent gaseous diffusion, are the main cause of the large standard deviation values of the links located close to the main emission sources (whose positions are indicated with the X marker in Fig. 4). Links 3, 7, and 9 exhibit the highest mean concentration values (column H1), since they lie nearby the main emission points. Instead, the lowest concentration values are recorded by links 14 and 15, not only because they lie farthest from the emission sources but also because the wind was blowing the emitted gases in other directions.

Concerning the measurement accuracy of each concentration sample, since the accounting confidence index is greater than 0.95, linear concentration measurements are affected by an error lower than 5%. Mean linear concentration is practically affected by the same relative error, since the resolution of the Rangefinder used to measure the link length is 1 m. This should be kept in mind when reading columns I and J, that refer anyway to “instantaneous” samples. The same columns give also an interesting indication about the space-time variation of the instantaneous link-averaged concentration: link 7 exhibits the maximum value of 1305 ppm, while link 9 has the minimum value (348 ppm), that can also be assumed as the background  $\text{CO}_2$  concentration level.

#### V. TOMOGRAPHIC RETRIEVAL OF $\text{CO}_2$ CONCENTRATION

As mentioned in the Introduction, a basic objective of this work is to apply the tomographic approach described in [2] to

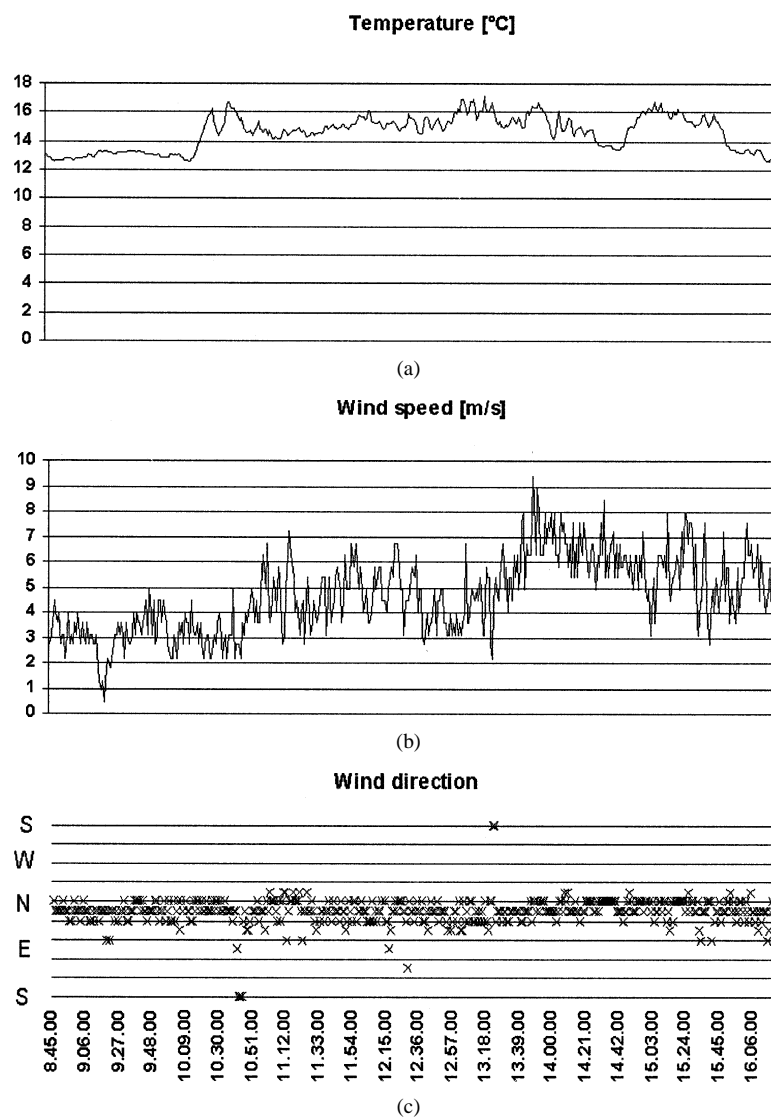


Fig. 5. Meteorological parameters acquired during the measurement campaign on November 20, 2001. From top to bottom: temperature, speed and direction of wind. The parameters are in minute average value.

process the set of average concentration measurements made along separate optical paths, to yield a 2-D concentration field estimate referred to the air volume interested by the ensemble of coplanar paths. In principle, if the 2-D field can be considered time-stationary over all links in the measurement interval, the specific network topology of Fig. 4 would guarantee good performance of the tomographic algorithm, in terms of coverage and spatial resolution of the reconstructed concentration field, independently of the measurement intervals adopted for each link. The ideal way to perform time-stationary measurements would have been to make simultaneous measurements along all links of the network, for a duration compatible with the time-stationarity hypothesis. As discussed in Section 2, in our case the need for a consistent network topology with the instrumentation at disposal led to a set of not simultaneous link measurements. However, measurements made in the same emission and weather conditions can be practically referred to a stationary 2-D concentration field pertinent to those conditions. For this reason, first a subset of measurements (both weather and concentration) characterized by the same wind direction

(NNE) was extracted from the whole dataset: as can be verified by comparing Fig. 5 with columns C and D of Table I, the NNE direction is common to all 15 links. The average wind velocity in the NNE direction, shown in Fig. 6, ranges from 3–5 m/s. Analyzing the time series of the concentration data of each link with the NNE wind condition (see Fig. 7), no evident drift of the mean value can be observed along any link. Therefore, though the wind velocity in the NNE direction cannot be considered perfectly stationary (Fig. 6), the mean CO<sub>2</sub> concentration measurements of the 15 time series of Fig. 7 can be considered as representative of a time-average concentration field over the monitored area, corresponding to an average wind speed of about 4 m/s blowing from NNE. These mean values are plotted in Fig. 8.

The concentration measurements were finally given as input to the tomographic algorithm: for its detailed description, the interested reader is referred to the original work where it was defined and utilized for the first time [9]. Here we simply recall that such algorithm is based on a stochastic approach that, after a preliminary random screening of possible solu-

TABLE I  
DATA REPORT OF THE CO<sub>2</sub> MEASUREMENT CAMPAIGN MADE ON NOVEMBER 20, 2001. A ROW CORRESPONDS TO ONE OF THE 15 LINKS OF THE NETWORK SHOWN IN FIG. 4. SEE SECTION IV FOR THE MEANING OF EACH COLUMN

A	B	C	D	E	F	G	H1	H2	I	J
	[m]	[hh:mm:ss]	[hh:mm:ss]	[sec]		[ppmm]	[ppm]	[ppm]	[ppm]	[ppm]
1	74	09:44:25	09:49:30	305	143	42775	578	65	467	821
2	71	09:50:00	09:57:30	450	230	40927	576	58	389	797
3	68	10:18:25	10:23:00	275	136	49766	733	111	350	939
4	66	10:23:40	10:31:45	485	265	34126	517	34	451	651
5	63	10:32:40	10:37:40	300	163	32419	515	37	458	667
6	65	10:45:00	10:47:20	140	71	30142	464	57	388	697
7	45	11:18:38	11:24:55	377	177	33625	747	140	410	1305
8	57	11:26:39	11:32:11	332	132	30299	532	57	388	761
9	72	11:43:15	11:48:49	334	176	50874	707	121	348	1018
10	75	11:50:25	11:54:06	221	110	44340	591	93	425	832
11	80	12:00:15	12:12:28	733	184	48044	601	72	478	833
12	86	12:12:58	12:19:54	416	230	49315	573	84	432	849
13	99	12:33:41	12:41:38	477	230	60778	614	76	452	835
14	72	12:42:16	12:47:06	290	160	39201	544	68	460	828
15	61	13:04:50	13:09:06	256	134	30929	507	46	436	708

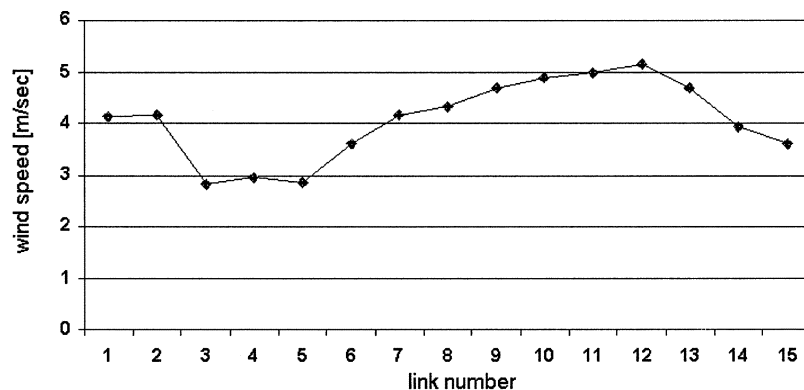


Fig. 6. Average wind speed in NNE direction.

tions, followed by an iterative optimization phase, retrieves the concentration field as a linear combination of a limited number (not more than ten) of Gaussian-shaped functions. Notice that the objective of the optimization phase is to minimize an error function that is practically the average rms error of the linear concentrations computed along each link (and corresponding to the attenuation in the original algorithm—[9, p. 2540]). Since the posed tomographic reconstruction problem is ill-conditioned in all practical cases (due to the low number of links available and/or to the network topology), the random algorithm generates a number of solutions that can be considered as equivalent in terms of the residual error (see [9,

p. 2541]). In general, equivalent solutions may correspond to different 2-D shapes of the reconstructed field, depending on measurements and network topology. For data reported in this paper, negligible discrepancies could be noticed among the equivalent solutions generated by the algorithm. Therefore, we report and discuss here the solution with the minimum error.

In particular, Fig. 9 plots the tomographic reconstruction, while in Fig. 10 is plotted the residual concentration error along the 15 links. The reconstructed field shows two significant concentration maxima located close to the end of link 8 and of the pair of links 5 and 6. This is in accordance with the measurement set, since links 3, 7, and 9 exhibit the highest

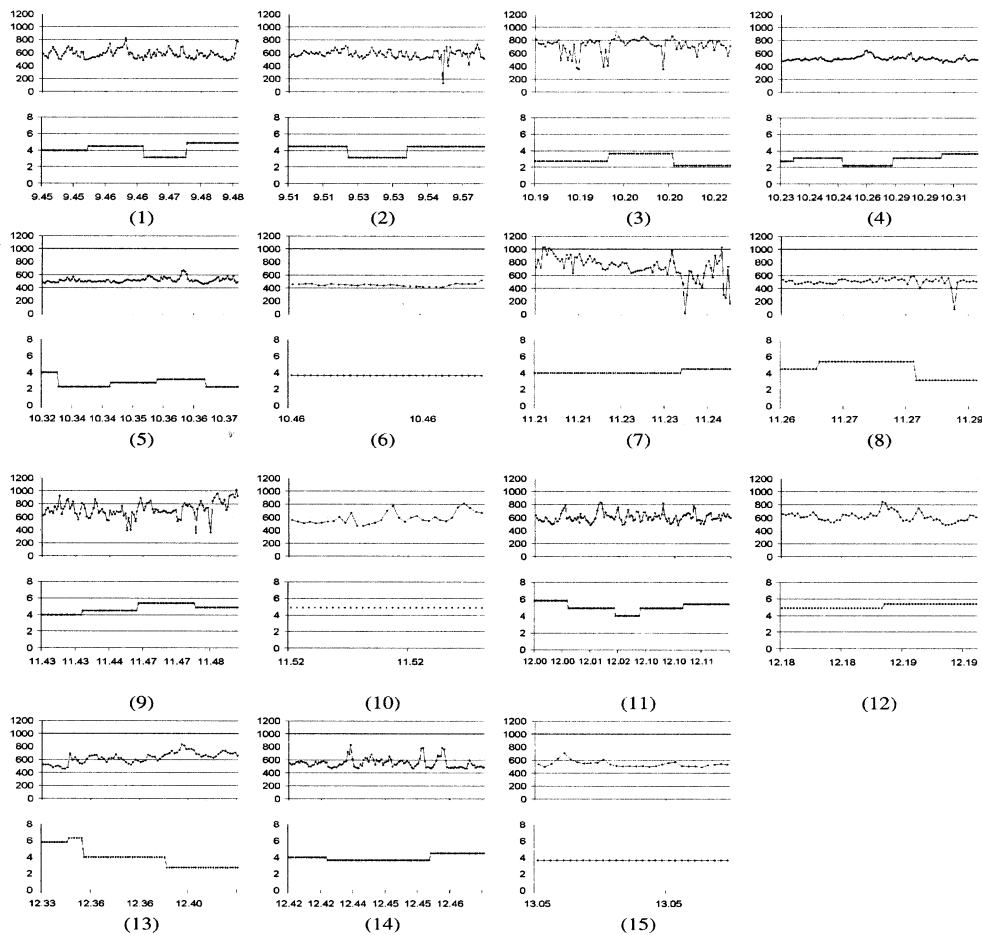


Fig. 7. Time series of the mean concentration values measured along each link (1–15), when wind is blowing from NNE. For each link, the concentration in parts per million (ppm), and the wind speed in meters per second (m/s) are reported, respectively, on the top and on the bottom of the subplot.

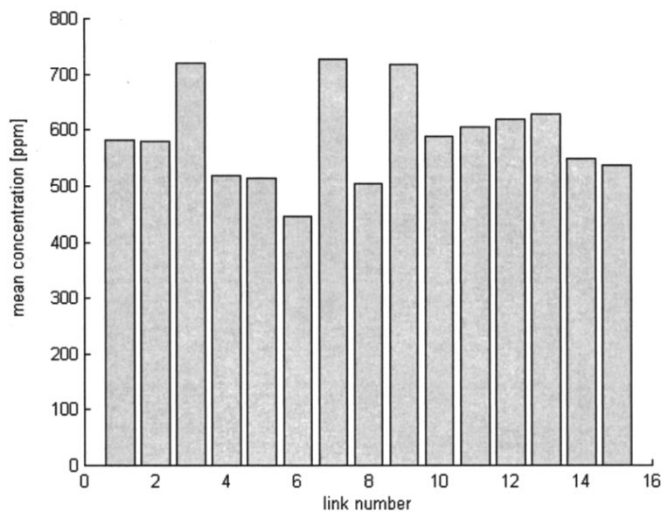


Fig. 8. Bar plot of the CO<sub>2</sub> time-averaged concentrations corresponding to the each of the 15 links pertinent to the subplots of Fig. 7.

mean concentrations (see Fig. 8). From a qualitative point of view, the positions of such maxima, though close to the border of the measurement network, are decidedly compatible with the position of the two main emission sources and of the

wind direction: in fact, the wind is blowing from NNE and the maxima are placed downstream with respect to the emission points.

From a quantitative point of view, instead, one could object that the mean concentrations of Fig. 8 (about 740 ppm) are not compatible with the point concentration values 2-D reconstruction: we refer in particular to the 7000 ppm peaks of Fig. 9. However, one can also notice that links with maximum mean concentrations are number 3, 7, and 9; thus, it is expected that around such links the 2-D field exhibits the maximum concentration. On the other hand, maxima could not be positioned along links 1, 2, 4, 5, 6, 8, 14, and 15, since they exhibit the lowest concentration values. Therefore, the only possible position where the two maxima could be placed by the algorithm is south of links 3, 7, and 9. Furthermore, so high local concentration values were confirmed by preliminary instrumentation tests made 50 cm over one emission source along a single 1-m length link, obtaining linear concentration values higher than 12 000 ppm. Based on such observations, it can be concluded that while the 2-D reconstructed field is qualitatively correct, the absence of additional links covering that southern border likely degraded the point accuracy with respect to that obtainable if wind had been blowing along the opposite direction.

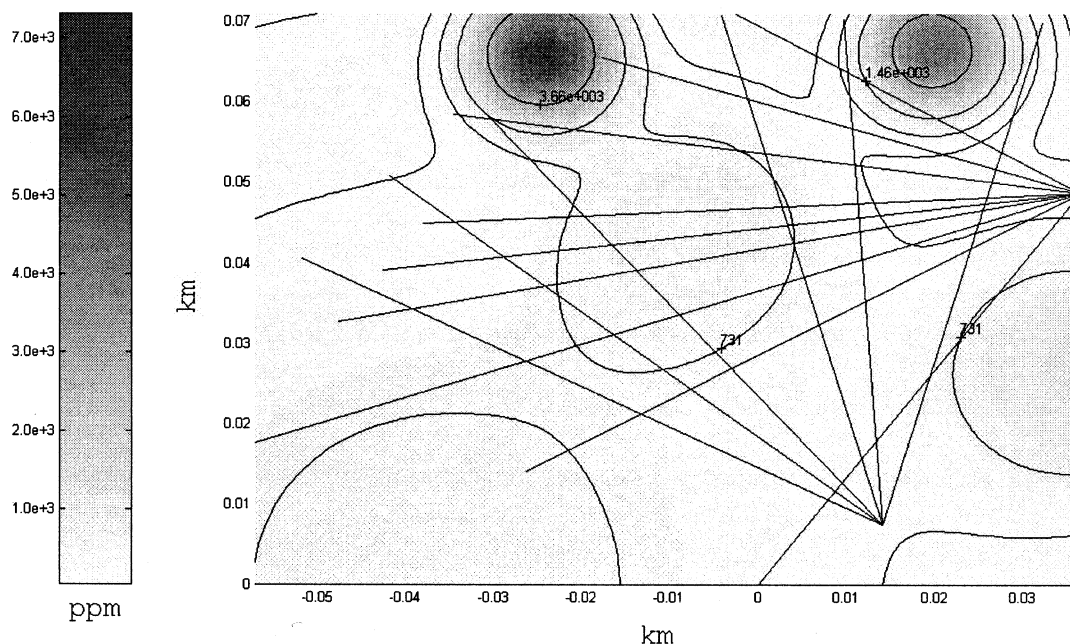


Fig. 9. Tomographic reconstruction of the 2-D mean concentration field of  $\text{CO}_2$  based on the mean concentration shown in Fig. 8.

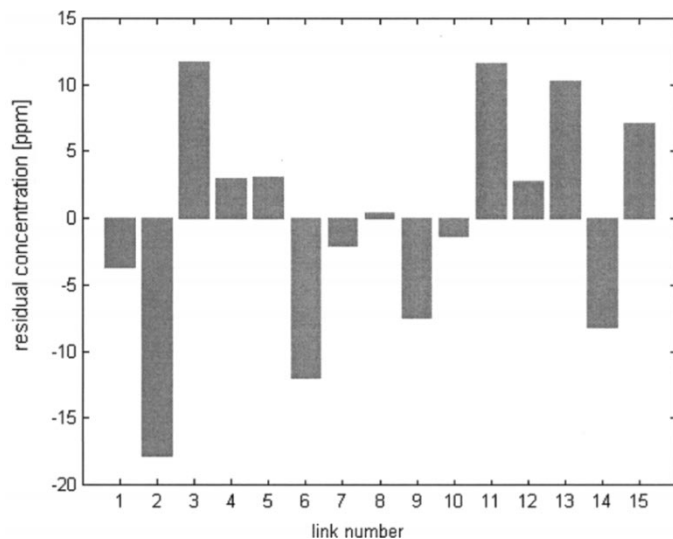


Fig. 10. Residual concentration values on the 15 links with the reconstruction shown in Fig. 9.

## VI. CONCLUSION

For the first time, an experiment was carried out with an IR laser system for the measurement of the atmospheric  $\text{CO}_2$  linear concentration over a volcanic area. The available instrumentation allowed to collect  $\text{CO}_2$  linear concentrations along a number of optical links placed over the emission area jointly with weather parameters. Due to the limited number of available devices (transmitter laser and retroreflectors), a particular measurement procedure and a preprocessing data selection phase was followed in order to apply a tomographic processing algorithm. Given the stationarity of the emission sources, such a procedure has permitted to define average  $\text{CO}_2$  concentrations along each link that could be referred to average atmospheric

conditions over a 3-h period. Therefore, the  $\text{CO}_2$  concentration field retrieved by tomographic processing could be associated to the same average conditions.

Indeed, a main issue would be to assess the tomographic reconstruction performance in such a volcanic environment. A reliable performance analysis would require independent 2-D fields at higher resolution: lidar or a dense point sampling system could solve this problem, but it is also evident that cost and complexity make this solution not practically exploitable in outdoor experiments. Therefore, the results obtained in this work should be considered somewhat qualitative: nevertheless, they are very promising, since they show that it is possible to remotely sense atmospheric gases using portable open path IR laser systems in limited extension areas, especially in applications requiring real-time operations: in such cases, in fact, the linear concentration data must be collected as quickly as possible and a multipath laser system would be desirable. One possible solution for a multipath system could be for instance that sketched in [10], even if its implementation appears quite complicated in outdoor environment. In alternative, the links of the measurement network could be scanned using a quick computer-based pointing system. In this way, it would be possible to perform real time monitoring over the whole area covered by the tomographic network, since this would provide time sequences of "snapshot" reconstructions of  $\text{CO}_2$  concentration fields.

## ACKNOWLEDGMENT

The authors wish to thank L. Capannesi for his technical support and E. Thornton and H. Adam (Boreal Laser, Inc.) for their cooperation. The authors would also thank an anonymous reviewer for suggestions.



## REFERENCES

- [1] A. C. Drescher, A. J. Gadgil, P. N. Price, and W. W. Nazaroff, "Novel approach for tomographic reconstruction of gas concentration distributions in air—Use of smooth basis functions and simulated annealing," *Atmos. Environ.*, vol. 30, no. 6, pp. 929–940, Mar. 1996.
  - [2] F. Cuccoli, L. Facheris, S. Tanelli, and D. Giuli, "Infrared tomographic system for monitoring the two-dimensional distribution of atmospheric pollution over limited areas," *IEEE Trans. Geosci. Remote Sensing*, vol. 38, pp. 1922–1935, July 2000.
  - [3] M. Carapezza *et al.*, "CO<sub>2</sub> and H<sub>2</sub>S concentrations in the atmosphere at the solfatara of pozzuoli," *Bull. Volcanol.*, vol. 47-2, pp. 287–293, 1984.
  - [4] G. Chiodini *et al.*, "Soil CO<sub>2</sub> flux measurements in volcanic and geothermal areas," *Appl. Geochem.*, vol. 13, no. 5, pp. 543–552, 1998.
  - [5] *GasFinder 2.0, Portable System, Operation Manual*.
  - [6] L. S. Rothman *et al.*, "The 1996 HITRAN molecular spectroscopic database and HAWKS (HITRAN atmospheric workstation)," *J. Quant. Spectrosc. Radiat. Transf.*, vol. 60, no. 5, pp. 665–710, Nov. 1998.
  - [7] J. Tulip, "Gas Detector," U.S. Patent 5 637 872, June 1997.
  - [8] —, "Gas Detector with Reference Cell," U.S. Patent 6 121 627, Jan. 2001.
  - [9] D. Giuli, L. Facheris, and S. Tanelli, "Microwave inversion technique based on stochastic approach for rainfall field monitoring," *IEEE Trans. Geosci. Remote Sensing*, vol. 37, pp. 2536–2555, Sept. 1999.
  - [10] M. L. Fischer *et al.*, "Rapid measurements and mapping of tracer gas concentrations in a large indoor space," *Atmos. Environ.*, vol. 35, pp. 2837–2844, 2001.
- Claudio Belotti** received the laurea degree in electronic engineering from the University of Florence, Florence, Italy, in 2001. Since 2002, he has been pursuing the Ph.D. degree in "Methods and technologies for environmental monitoring" at the Department of Electronics and Telecommunications, University of Florence, here he works with the Radio-communications Laboratory team. His main research activity is data processing for atmospheric remote sensing applications.
- Fabrizio Cuccoli** received the laurea degree (cum laude) in electronic engineering from the University of Florence, Florence, Italy, in 1996, and the Ph.D. degree in methods and technologies for environmental monitoring from the Università della Basilicata, Potenza, Italy, in 2001.
- Since 2000, he has been a Research Scientist for the Consorzio Nazionale Interuniversitario delle Telecomunicazioni (CNIT) at the Dipartimento di Elettronica e Telecomunicazioni, University of Florence, where he works with the Radar and Radiocommunications Laboratory team. His main research activity is in the area of remote sensing of rainfall, water vapor, and atmospheric gaseous components through active systems (e.g., meteorological radar, infrared, and microwave devices). His current interest is the microwave and infrared spectral analysis of absorption characteristics of the atmosphere components and related attenuation measurements for data processing.
- Luca Facheris** received the laurea degree (cum laude) in electronic engineering from the University of Florence, Florence, Italy, in 1989, and the Ph.D. degree in electronic and information engineering from the University of Padua, Padua, Italy, in 1993.
- Since 1993, he has been with the Department of Electronic Engineering, University of Florence, where he is currently an Assistant Professor in the telecommunications area. His main research activity is in the area of signal and data processing for active remote sensing: radar polarimetry, ground and spaceborne weather radars, and methods for the exploitation of attenuation measurements at microwaves and infrared for remote sensing of the atmosphere.
- Orlando Vaselli** received the laurea degree in geological sciences from the University of Florence, Florence, Italy, in 1985.
- In 1990, he became the Head of the Atomic Absorption Spectrophotometry Laboratory, and in 1997, he became a Lecturer in geochemistry and volcanology at the Department of Earth Sciences, University of Florence. Since November 2001, he has been an Associate Professor at the same department in the University of Florence. After dealing from 1990 to 1995 with mantle rock geochemistry, his main research is presently related to the geochemical investigation of fluid discharges in volcanic environment.
- Mr. Vaselli was awarded by the Europrobe (PANCARDI) for his scientific activity in the Pannonian-Carpathian Region, in 1999. He received three fellowships from the Royal Academy of London and Italian National Research Center (CNR), in 1991, 1993, and 1995, respectively.